Atomic kinetic energy, momentum distribution, and structure of solid neon at zero temperature

C. Cazorla[1,2] and J. Boronat[3]
[1]*London Centre for Nanotechnology, UCL, London WC1H OAH, United Kingdom*
[2]*Department of Physics and Astronomy, UCL, London WC1E 6BT, United Kingdom*
[3]*Departament de Física i Enginyeria Nuclear, UPC, Campus Nord B4-B5, Barcelona E-08034, Spain*
(Received 9 October 2007; published 30 January 2008)

We report on the calculation of the ground-state atomic kinetic energy E_k and momentum distribution of solid Ne by means of the diffusion Monte Carlo method and Aziz HFD-B pair potential. This approach is shown to perform notably for this crystal since we obtain very good agreement with respect to experimental thermodynamic data. Additionally, we study the structural properties of solid Ne at densities near the equilibrium by estimating the radial pair-distribution function, Lindemann's ratio, and atomic density profile around the positions of the perfect crystalline lattice. Our value for E_k at the equilibrium density is 41.51(6) K, which agrees perfectly with the recent prediction made by Timms *et al.*, 41(2) K, based on their deep-inelastic neutron scattering experiments carried out over the temperature range 4–20 K, and also with previous path integral Monte Carlo results obtained with the Lennard-Jones and Aziz HFD-C2 atomic pairwise interactions. The one-body density function of solid Ne is calculated accurately and found to fit perfectly, within statistical uncertainty, to a Gaussian curve. Furthermore, we analyze the degree of anharmonicity of solid Ne by calculating some of its microscopic ground-state properties within traditional harmonic approaches. We provide insightful comparison to solid ^{4}He in terms of the Debye model in order to assess the relevance of anharmonic effects in Ne.

DOI: 10.1103/PhysRevB.77.024310 PACS number(s): 61.50.Ah, 67.80.−s, 67.90.+z

I. INTRODUCTION

Noble gases like He, Ne, Xe, and Ar have been intensively studied during the last decades, both experimentally and theoretically.[1–3] Due to their simple electronic closed-shell structure, they appear to be affordable many-body systems where to carry out feasible quantum computations and test methods of calculation. Even though most of them are regarded as classical systems, microscopic quantum approaches are required to understand the behavior of the lighter ones, He and Ne, at low temperatures. As it is well known, He is the most representative of the quantum many-body systems. Unique features like Bose-Einstein condensation and superfluidity take place in the liquid at a few K, and recently several experimental groups have detected superfluid signal in the solid phase in the mK range,[4,5] a signal that in the homogeneous crystal has been ruled out by accurate theoretical calculations.[6,7] Moreover, the atomic momentum distribution $n(\mathbf{k})$ of ^{4}He differs significantly from those of classical systems, leading to a non-Gaussian $n(\mathbf{k})$ curve sharply peaked around $k=0$.[8–10] The reasons for those phenomena to happen in helium are the light mass of the atoms, bosonic nature of the system, and weakness of the interparticle interactions. On the other side, Ne has long attracted the interest of condensed-matter scientists since it is an intermediate quantum system which provides valuable physical insight when compared to other quantum and classical systems. Indeed, the De Boer quantum parameter[11] defined as

$$\Lambda^* = \frac{h}{\sqrt{m\epsilon\sigma^2}}, \tag{1}$$

where m, ϵ, and σ are the atomic mass, energy scale of the atomic interactions, and typical interatomic distance of the system, respectively, amounts to 0.54 in Ne (2.50 in ^{4}He) while in Ar and other heavier noble gases, where classical behavior is expected, it drops significantly to zero. Essentially, the quantum character of liquid and solid Ne is evidenced in their atomic kinetic energies and momentum distributions, which differ appreciably from the predictions made by classical statistical mechanics. Accordingly, anharmonic effects in the crystal may develop important at low temperatures due to the large zero-point motion of the atoms.[12]

In this work, we study solid Ne at zero temperature by means of the diffusion Monte Carlo (DMC) method[13–15] and the Aziz HFD-B pair potential.[16] Our approach is microscopic and *exact* in the sense that the total and partial ground-state energies of the crystal may be calculated within statistical uncertainty only. There are a burdensome amount of theoretical and experimental papers dealing with the thermodynamics and lattice dynamics of solid neon; however, numerical results for the atomic kinetic energy are not so abundant. By the beginning of the 1960s, Bernades[17] and Nosanow and Shaw[18] were the first in attempting to estimate E_k theoretically. They used uncorrelated single-particle wave functions within the variational and Hartree approaches, respectively, and arrived at reasonable values not too far from present-day calculations; however, the binding energies that they reported were in significant disagreement with experimental data. These results made evident the need of improved theoretical schemes to account for the atomic correlations in Ne. A few years after the work of Bernades and Nosanow, Koehler estimated E_k=42.6 K by means of the self-consistent phonon (SCP) approach, improving mildly the agreement with experiments.[19]

On the experimental side, however, it was not until the beginning of the 1980s, with the development of the deep-inelastic neutron scattering technique (DINS), that direct measurement of E_k in the condensed phases of matter became accessible. Peek *et al.* performed the first measurements in solid Ne, covering the temperature interval

4.5–26.5 K.[20] The authors of the first study reported $E_k = 49.1 \pm 2.8$ K for the ground-state kinetic energy, and because of the large discrepancies with respect to calculations based on harmonic models, they suggested substantial anharmonic effects in solid Ne.

Reassuringly, a few years after the measurements of Peek *et al.*,[20] theoretical estimations by Asger and Usmani,[21] who used a perturbational approach based on a Wigner-Kirkwood high-temperature expansion with the Lennard-Jones (LJ) and Aziz (Ref. 24) pair potentials, amounted to $E_k \sim 49$ K at temperatures near 10 K. Regardless, previous to the results of Asger *et al.*,[21] Cuccoli and co-workers[22] arrived at kinetic energies ~ 7 K below the results of Peek *et al.*, based on the full quantum path integral Monte Carlo (PIMC) approach and the LJ interaction. The authors of this work suggested that their disagreement with the results of Peek *et al.* could be in part due to the oversimplification of the atomic interactions made by the adopted potential. Subsequently, Timms *et al.*[23] performed a series of new low-temperature DINS experiments in solid Ne at high momentum tranfers with an improved experimental setup. They found very good agreement with Cuccoli *et al.*[22] and also with Timms *et al.*,[23] who performed an exhaustive PIMC study of the crystal at low temperatures using both LJ and HFD-C2 pair potentials. In addition, a recent theoretical study by Neumann and Zoppi, in which computational techniques and interatomic potentials similar to those of Ref. 23 are used, comes to reinforce the accuracy of the data of Timms *et al.*[25] Very recently, Timms *et al.*[26] have reported new additional DINS measurements in solid Ne performed within the temperature range 4–20 K. By doing this, they complement their previous results and provide a truster way to infer the value of E_k in the groundstate, which by means of extrapolation of the excess kinetic energy turns out to be 41(2) K.

In the present work, we report quantum Monte Carlo results of the equation of state and other thermodynamic properties of solid Ne over a range of densities near equilibrium ($-1.2 \leq P \leq 6$ kbar) and find overall excellent agreement with experimental data. Structural properties of the crystal—namely, the radial pair-distribution function $g(r)$, atomic density profile around the positions of the perfect crystalline lattice (sites), and Lindemann ratio—are also provided. Remarkably, we estimate accurately the atomic kinetic energy of the crystal at its equilibrium density by means of the pure estimator technique within the DMC approach.[27–29] Our result $E_k = 41.51(6)$ K is in very good agreement with the recent prediction of Timms *et al.*[26] We have also calculated the ground-state atomic momentum distribution $n(\mathbf{k})$ of solid Ne, and it is found to fit perfectly to a Gaussian within the statistical uncertainty.

Additionallly, we have analyzed the degree of anharmonicity of solid Ne in its ground state. With this aim, we have computed the atomic kinetic energy and mean-squared displacement within the self-consistent average phonon (SCAP) approach,[27,28] which is a simplified version of the self-consistent phonon method[29] that has proved successful in reproducing a deal of thermodynamic properties of rare gas solids. We find the SCAP results are not in full agreement with the quantum DMC ones, thus revealing this approach might not allow for an accurate description of Ne at the microscopic level. In a further step, we devise an harmonic model based on the HFD-B potential in which the interaction between particles depends on their relative distances, equilibrium positions, and the force constant field (second derivatives of the potential energy evaluated in the perfect crystal configuration). By using the DMC approach, we calculate the total and kinetic energies associated with this model and find significant discrepancies with respect to the full HFD-B results. According to these outcomes, solid Ne may be regarded as a *moderate* anharmonic crystal since, contrarily to what is observed in solid ^{4}He, its $n(\mathbf{k})$ does not deviate appreciably from the Gaussian pattern.

The remainder of this article is as follows. In Sec. II, we describe the computational techniques and models that have been used on this study. Next, in Sec. III, we present our results and compare to previous experimental and theoretical data. In Sec. IV, we finalize by summarizing the main conclusions, giving some general remarks.

II. TECHNIQUES AND MODEL

A. Diffusion Monte Carlo method

The DMC method is a zero-temperature method which provides the exact ground-state energy of the many-boson interacting systems within some statistical errors.[13–15] This technique is based on a short-time approximation for the Green's function corresponding to the imaginary time-dependent Schrödinger equation, which is solved up to a certain order of accuracy within an infinitesimal interval $\Delta\tau$. Despite this method being algorithmically simpler than the domain Green's function Monte Carlo method,[15,30] it presents some $(\Delta\tau)^n$ bias coming from the factorization of the imaginary time propagator $e^{-(\Delta\tau/\hbar)H}$. Nevertheless, our implementation of DMC is quadratic;[31] hence, the control of the time-step bias is efficiently controlled since the required $\Delta\tau \to 0$ extrapolation is nearly eliminated by choosing a sufficiently small time step. The Hamiltonian H describing our system is

$$H = -\frac{\hbar^2}{2m_{\mathrm{Ne}}}\sum_{i=1}^{N}\nabla_i^2 + \sum_{i<j}^{N} V_2(r_{ij}), \tag{2}$$

where m_{Ne} is the mass of a Ne atom, r_{ij} the distance between atoms composing an i,j pair, and $V_2(r_{ij})$ the interatomic interaction that we have chosen as the Aziz HFD-B potential.[16] The corresponding Schrödinger equation in imaginary time ($it \equiv \tau$),

$$-\hbar\frac{\partial\Psi(\mathbf{R},\tau)}{\partial\tau} = (\mathrm{H} - E)\Psi(\mathbf{R},\tau), \tag{3}$$

with E an arbitrary constant, can be formally solved by expanding the solution $\Psi(\mathbf{R},\tau)$ in the basis set of the energy eigenfunctions $\{\Phi_n\}$. It turns out that $\Psi(\mathbf{R},\tau)$ tends to the ground-state wave function Φ_0 of the system for an infinite imaginary time as well as the expected value of the Hamiltonian tending to the ground-state value E_0. The Hermiticity of the Hamiltonian guarantees the equality

$$E_0 = \frac{\langle \Phi_0 | \mathrm{H} | \Phi_0 \rangle}{\langle \Phi_0 | \Phi_0 \rangle} = \frac{\langle \Phi_0 | \mathrm{H} | \psi_T \rangle}{\langle \Phi_0 | \psi_T \rangle} = \langle H \rangle_{DMC}, \tag{4}$$

where ψ_T is a convenient trial wave function which depends on the atomic coordinates of the system $\mathbf{R} \equiv \{\mathbf{r}_1, \mathbf{r}_2, \ldots, \mathbf{r}_N\}$. Consequently, the ground-state energy of the system can be computed by calculating the integral

$$\langle \boldsymbol{H} \rangle_{DMC} = \lim_{\tau \to \infty} \int_V E_L(\mathbf{R}) f(\mathbf{R}, \tau) d\mathbf{R}, \tag{5}$$

where $f(\mathbf{R}, \tau) = \Psi(\mathbf{R}, \tau)\psi_T(\mathbf{R})$ and $E_L(\mathbf{R})$ is the local energy defined as $E_L(\mathbf{R}) = \mathrm{H}\psi_T(\mathbf{R})/\psi_T(\mathbf{R})$. The introduction of $\psi_T(\mathbf{R})$ in $f(\mathbf{R}, \tau)$ is known as importance sampling, and it certainly improves the way in which integral (5) is computed [for instance, by imposing $\psi_T(\mathbf{R}) = 0$ when r_{ij} is smaller than the core distance of the interatomic interaction].

In this work, all the operators diagonal in real space which do not commute with the Hamiltonian—that is, $[H, \hat{O}] \neq 0$—have been sampled with the pure estimator technique.[32–34] With this method, essentially, the possible bias induced by ψ_T in the mixed estimator $\langle \Phi_0 | \hat{O} | \psi_T \rangle$ is removed by proper weighting of the configurations along the simulation.

B. Trial wave function and pair potential

We have modeled solid Ne by assuming pointlike atoms interacting via a radial pairwise potential and with equilibrium positions distributed according to the fcc structure. Neon is observed to remain stable in the fcc structure up to pressures of 1100 kbar and at ambient temperature;[35] therefore, no other configuration apart from this has been considered in the present study. The potential chosen for the interatomic interactions is the semiempirical Aziz HFD-B one,[16] which has proved excellent in reproducing some of the macroscopic and microscopic properties of Ne over a wide range of temperature and pressure,[36] and appears to be more realistic than the Aziz (Ref. 24), and LJ models at short distances. Explicitly,

$$V(r) = \epsilon \Theta(x), \tag{6}$$

where

$$\Theta(x) = A \exp(-\alpha x + \beta x^2) - F(x)\left(\frac{C_6}{x^6} + \frac{C_8}{x^8} + \frac{C_{10}}{x^{10}}\right)$$

and

$$F(x) = \begin{cases} \exp\left[-\left(\frac{D}{x} - 1\right)^2\right], & x < D, \\ 1 & x \geq D. \end{cases}$$

The value of the parameters of the potential are $A = 895\,717.95$, $\alpha = 13.864\,346\,71$, $D = 1.36$, $r_m = 3.091$ Å, $\beta = -0.129\,938\,22$, $\epsilon = 42.25$ K, $C_6 = 1.213\,175\,45$, $C_8 = 0.532\,227\,49$, and $C_{10} = 0.245\,707\,03$, with $x \equiv r/r_m$. It is known that, upon high pressure, the introduction of additional terms in the effective atomic potentials of rare gases is required to account for many-body effects taking place in them; for instance, in solid Ar this limit is posed around 50 kbar.[37,38] This circumstance, however, does not affect the reliability of the results that we are to present shortly, since the pressure range involved in our simulations is $-1.2 \leq P \leq 6$ kbar.

Regarding the trial wave function chosen for importance sampling, ψ_T, we have adopted the extensively used and tested Nosanow-Jastrow model,[39–41]

$$\psi_T(\mathbf{r}_1, \mathbf{r}_2, \ldots, \mathbf{r}_N) = \prod_{i \neq j}^{N} \mathrm{f}_2(r_{ij}) \prod_{i=1}^{N} \mathrm{g}_1(|\mathbf{r}_i - \mathbf{R}_i|), \tag{7}$$

with $\mathrm{f}_2(r) = e^{-(br)^c/2}$ solids and $\mathrm{g}_1(r) = e^{-ar^2/2}$. The best parameter values are $a = 6.5$ Å^{-2}, $b = 4.0$ Å, and $c = 5.0$, optimized using the variational Monte Carlo method. Their dependence with the pressure is small and therefore neglected for its use in the DMC simulations. The first factor in ψ_T accounts for the correlations between particles induced by the interactions, while the second enforces the atomic ordering within the system by attaching each particle to one site of the perfect lattice through a Gaussian function. The indistinguishability of the Ne atoms has been neglected throughout this work since the Nosanow-Jastrow model is not symmetric under the exchange of particles. This choice is fairly justified since quantum effects derived from a correct symmetrization are not expected to play any significant role in the solid properties calculated in this work. In fact, the same conclusion for the same quantities also holds for solid ^{4}He, a solid with a larger quantum behavior. The parameters of the simulation—namely, the number of particles per box, time step, and target walker population (that is, the mean number of walkers along the simulation)—have been chosen in order to ensure the correct asymptotic behavior; their respective values are $N = 256$, $\Delta\tau = 2.7 \times 10^{-4}$ K^{-1}, and $n_w = 260$.

At each density, finite-size effects have been corrected by including the tails of the kinetic and potential energies into the total energy, both estimated assuming $g(r) = 1$ beyond half the length of the simulation box. This assumption could be too crude for solids (see Fig. 2), and therefore we have checked the reliability of this approximation in our system. To this end, we have carried out some simulations with 500 atoms and compared the energetic and structural results with the ones obtained for a box of 256 particles at the same density. For instance, at a density $\rho = 0.045$ Å^{-3} the energies are $E/N = -238.88(4)$ K and $-238.69(8)$ K and the Lindemann ratios $\gamma_{\mathrm{Ne}} = 0.077(1)$ and $0.079(3)$ for $N = 256$ and 500 particles, respectively. The differences observed are therefore not significant within our statistical uncertainty, and the size corrections are reasonably included.

III. RESULTS

A. Thermodynamic properties

In Fig. 1 we show our results for the total atomic energy of solid Ne at zero temperature. The solid line in it corresponds to the polynomial curve $e(\rho) = E(\rho)/N$,

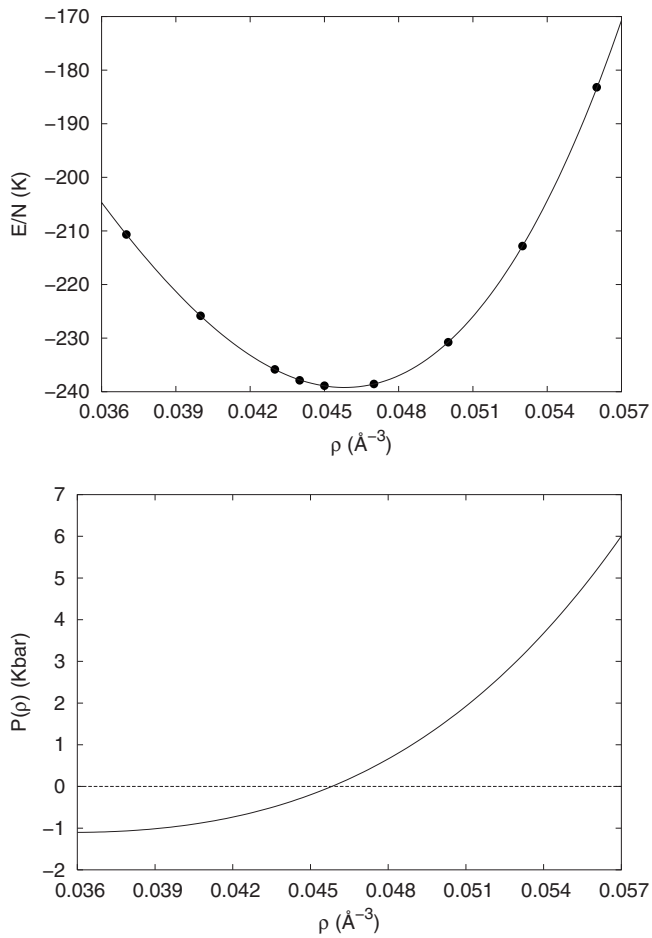

FIG. 1. Top: energy versus density for solid Ne at zero temperature. The solid line corresponds to the polynomial curve of Eq. (8) and the dots to the calculated DMC total energies per particle; errors bars are smaller than the size of the symbols. Right: equation of state of solid Ne at zero temperature computed with the DMC method and the Aziz HFD-B potential.

$$e(\rho) = e_0 + a\left(\frac{\rho - \rho_0}{\rho_0}\right)^2 + b\left(\frac{\rho - \rho_0}{\rho_0}\right)^3, \tag{8}$$

which has been fitted to the DMC energies reported in Table I (solid points in the figure). The values of the parameters of the best fit are $a=938(3)$ K, $b=871(20)$ K, $e_0=-239.21(3)$ K, and $\rho_0=0.045\,82(2)$ Å^{-3}, where e_0 and ρ_0 are the equilibrium energy per particle and density, respectively. The agreement between our results and experiments is reasonably good for energy $e_0^{expt}=-232(1)$ K and density $\rho_0^{expt}=0.0449\,76(3)$ Å^{-3}.[42,43]

Once $e(\rho)$ is known, it is straightforward to deduce the pressure $P(\rho)$ (see Fig. 1), and compressibility $\kappa(\rho)$ of the system at any density through the relations

$$P(\rho) = \rho^2 \frac{\partial e(\rho)}{\partial \rho},$$

$$\kappa(\rho) = \frac{1}{\rho}\frac{\partial \rho}{\partial P}. \tag{9}$$

TABLE I. Total, potential, and kinetic energies per particle of solid Ne at absolute zero as computed with the DMC method and the pure estimator technique. Energies are in units of K.

ρ (Å^{-3})	E/N	E_p/N	E_k/N
0.040	−225.84(4)	−256.26(8)	30.34(8)
0.043	−235.83(4)	−272.04(8)	36.23(8)
0.044	−237.88(4)	−276.50(8)	38.57(8)
0.045	−238.88(4)	−279.43(8)	40.61(8)
0.047	−238.55(4)	−283.76(8)	45.17(8)
0.050	−230.76(4)	−282.81(8)	52.17(8)
0.053	−212.83(4)	−272.15(8)	59.31(8)
0.056	−183.20(4)	−249.61(8)	66.41(8)

The compressibility at the equilibrium density that is obtained, $\kappa_0=0.084(4)$ kbar^{-1}, compares excellently to the experimental value $\kappa_0^{expt}=0.089(2)$ kbar^{-1}.[43]

An interesting magnitude in the study of condensed phase systems is the spinodal density ρ_S, which is the thermodynamical limit for the system to remain in a homogeneous phase. At this density, the relation $\partial P/\partial\rho=0$ is fulfilled, which is equivalent to requiring infinite compressibility or zero speed of sound in the system. Our prediction for ρ_S is $0.035\,75(5)$ Å^{-3}, which corresponds to a pressure $P(\rho_S)=-1.102(4)$ kbar. In Ref. 44, Herrero presents a comprehensive study of solid Ne at negative pressures by means of the PIMC method. The author models the interatomic interactions with the LJ potential and estimates the pressure at the spinodal density and zero temperature by means of a linear fit to the squared bulk modulus with respect to pressure; he obtains $P(\rho_S)^{PIMC}=-0.91$ kbar and $\rho_S^{PIMC}=0.0356$ Å^{-3}. The disagreement between this and our value for $P(\rho_S)$ can be explained in terms of the adopted interatomic potential, since small differences in the total energies may develop into large ones within successive derivatives.

B. Structural properties

We have explored several structural properties of solid Ne. In Fig. 2, we plot the averaged radial pair-distribution function $g(r)$, which is proportional to the probability of finding a particle at a certain distance r from another. According to what is expected in crystals, $g(r)$ emerges peaked with maxima corresponding to the distances between successive shells of atoms within the perfect lattice, though the peaks broaden with respect to the profiles which are obtained in classical solids.

A characteristic parameter in the study of quantum solids is the Lindemann's ratio γ, which is defined as the ratio between the squared root of the mean-squared displacement $\langle \mathbf{u}^2 \rangle$ and the distance between first nearest neighbors in the perfect crystalline lattice. Our estimation of the Lindemann's ratio at the equilibrium density (pure estimation) is $\gamma_{\mathrm{Ne}}=0.088(2)$, which is significantly smaller than in ^{4}He ($\sim$0.26) and H_2($\sim$0.18), but still larger than in classical solids at finite temperature and far from melting ($\sim$0.03). The

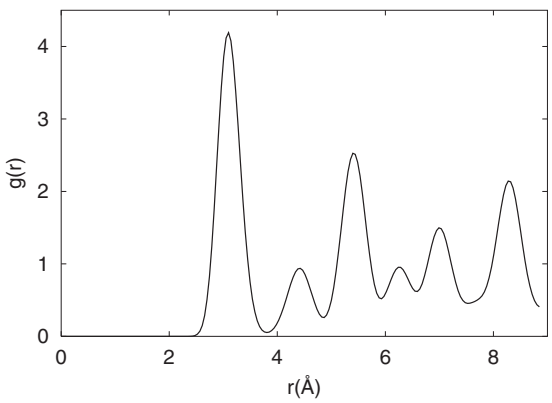

FIG. 2. Averaged radial pair-distribution function $g(r)$ of solid Ne at zero temperature and the equilibrium density.

corresponding mean-squared displacement $\langle \mathbf{u}_{\mathrm{Ne}}^2 \rangle$ amounts to 0.077(1) Å^2. In Table II, we quote the value of γ_{Ne} at several densities out of the equilibrium. As is observed therein, the general trend of γ_{Ne} is to reduce when the density is increased; this behavior is easily understood in terms of gain of cohesion energy, which must balance with the increasing of kinetic energy of the system arising from atomic localization.

Aimed at characterizing the spatial distribution of the atoms around the equilibrium positions in solid Ne, we have calculated the atomic density profile function (averaged for all directions) $\mu(r)$ and kurtosis ζ_Q. The averaged atomic density profile function $\mu(r)$ yields the probability of finding a particle at a distance within the interval $(r, r+dr)$ from any arbitrary site of the lattice. According to this definition, the mean-squared displacement $\langle \mathbf{u}^2 \rangle$ can be obtained as

$$\langle \mathbf{u}^2 \rangle = 4\pi \int_0^\infty \mu(r) r^4 dr. \tag{10}$$

In Fig. 3, we plot $\mu(r)$ at the equilibrium density (dots), together with the Gaussian curve that we have adjusted to it (solid line). To check the reliability of this fit, we have assumed the Gaussian curve in Eq. (10), instead of $\mu(r)$, and then recalculated $\langle \mathbf{u}^2 \rangle$. Proceeding so, we obtain 0.079(1) Å^2 which agrees perfectly with the direct calculation 0.077(1) Å^2. Next, we compute ζ_Q in several directions of the cubic cell so as to discern whether the atoms distribute

TABLE II. Lindemman's ratio γ_{Ne} and kurtosis ζ_Q of solid Ne at different densities close to equilibrium.

ρ(Å^{-3})	γ_{Ne}	$\zeta_{(100)}$	$\zeta_{(010)}$
0.040	0.099(2)	0.017(12)	0.012(14)
0.043	0.092(2)	0.000(8)	−0.001(8)
0.044	0.091(2)	0.000(10)	0.000(10)
0.045	0.087(2)	−0.006(7)	−0.014(7)
0.047	0.086(2)	0.000(20)	0.000(10)
0.050	0.083(2)	0.000(10)	−0.010(10)

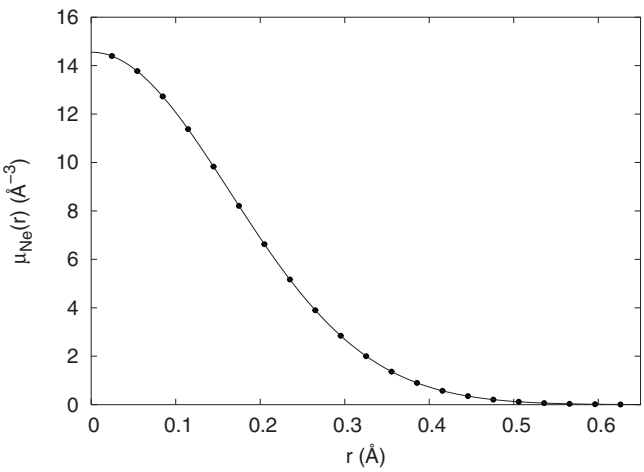

FIG. 3. Atomic averaged density profile $\mu(r)$ of solid Ne at zero temperature and the equilibrium density.

isotropically in average or not around the sites. The kurtosis is defined as

$$\zeta_{(ijk)} = \frac{\langle \mathbf{u}_{(ijk)}^4 \rangle}{\langle \mathbf{u}_{(ijk)}^2 \rangle^2} - 3, \tag{11}$$

where $\mathbf{u}_{(ijk)}$ are the projections of the position vectors which relate each lattice site to its nearest particle along the (ijk) direction (Cartesian basis). As is well known, if the atomic density distribution over the equilibrium positions is of Gaussian type, the kurtosis is null. In the case of solid Ne, we have obtained $\zeta_{(100)}$=0.0078(63) and $\zeta_{(010)}$=0.0062(59), which indeed might be regarded as values compatible with zero. Additional results for ζ_Q obtained with the pure estimator technique are quoted in Table II.

C. Kinetic energy and momentum distribution

In Table I, we summarize the value of the atomic ground-state kinetic and potential energies of solid Ne near equilibrium ($P \sim 0$). All the E_p and E_k results have been computed within the pure estimator technique and DMC method, and thus any possible errors associated with them are of statistical kind or stem from the modelization of the interatomic interactions. In particular, we have estimated E_k =41.51(6) K at the equilibrium density. In Fig. 4, we plot the values of the excess kinetic energy of solid Ne, defined as $E_{exc}=E_k-(3/2)T$, as measured by Peek *et al.*[20] and Timms *et al.*[26] within the temperature range 4–20 K. Therein, we also include estimations of E_{exc} as obtained with the PIMC approach over the same T interval, together with our ground-state result which is located at the ordinate axis. By performing linear fits to the excess kinetic energy, it is shown that our ground-state prediction is in very good agreement with the measurements of Timms *et al.*[26] and the PIMC estimations,[23] whereas not so with the results of Peek *et al.*[20] The causes for this disagreement may be explained, as has been suggested elsewhere,[25,26] in terms of systematic experimental errors, since the temperature dependence of E_{exc} ob-

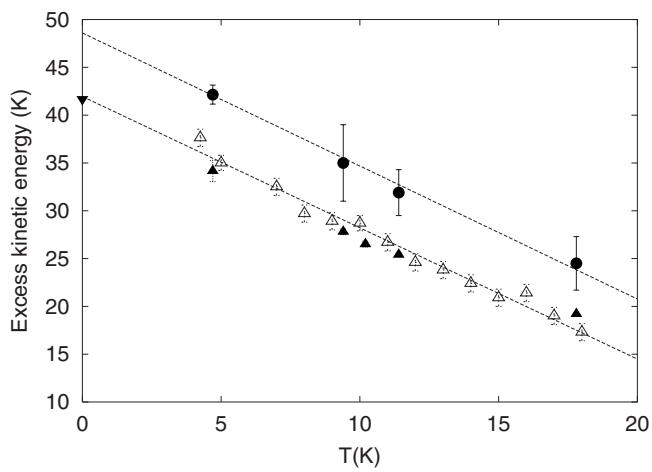

FIG. 4. Excess atomic kinetic energy of solid Ne at low temperatures. Experimental data of Ref. 26 are represented by △, measurements of Ref. 20 by ●, PIMC estimations of Ref. 23 by ▲, and our ground state estimation by ▼ (in the ordinate axis). The lines in the plot correspond to linear fits to the experimental data of Refs. 20 and 26.

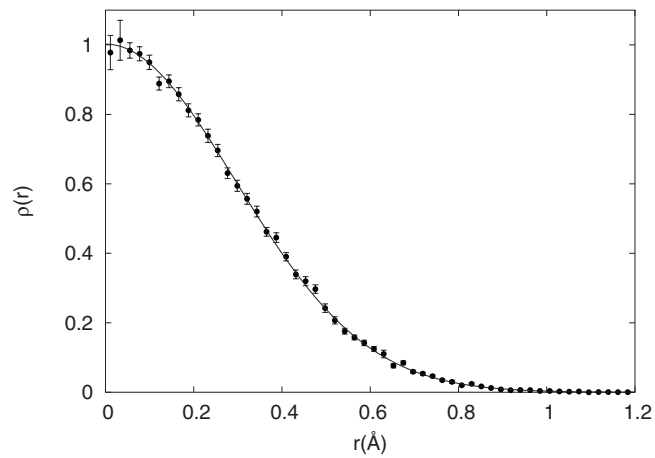

FIG. 5. One-body density matrix of solid Ne at the equilibrium density. The solid line in the figure corresponds to the Gaussian curve that we have fitted to the results.

tained by Peek and co-workers appears to coincide with the results of Timms *et al.* results. A likely explanation can rely on the range of neutron momentum transfers involved in those first DINS experiments, about two orders of magnitude less intense than in posterior measurements, which might not be sufficiently large so as to reach the high-Q regime required for the impulse approximation of the dynamic structure factor to be valid.[26]

Another physically rich quantity in the study of quantum liquids and solids is the one-body density matrix $\varrho(\mathbf{r},\mathbf{r}')$, which is defined as

$$\varrho(\mathbf{r},\mathbf{r}') = \langle \Phi_0 | \hat{\psi}^\dagger(\mathbf{r}) \hat{\psi}(\mathbf{r}') | \Phi_0 \rangle, \tag{12}$$

where $\hat{\psi}(\mathbf{r}')$ and $\hat{\psi}^\dagger(\mathbf{r})$ are, respectively, the field operators which destroy a particle from position $\mathbf{r}'$ and create one at position $\mathbf{r}$ and Φ_0 is the ground-state wave function. In boson systems the asymptote $\lim_{r\to\infty}\varrho(r)$ provides the condensate fraction of the associated homogeneous system n_0. The Fourier transform of $\varrho(r)$ is directly the atomic momentum distribution,

$$n(\mathbf{k}) = \rho \int d\mathbf{r}\, e^{i\mathbf{k}\cdot\mathbf{r}} \varrho(r). \tag{13}$$

In the quantum Monte Carlo formalism, the one-body density function can be estimated by averaging the coordinate operator $A(\mathbf{r},\mathbf{r}_1,\ldots,\mathbf{r}_N) \equiv \psi_T(\mathbf{r}_1+\mathbf{r},\mathbf{r}_2,\ldots,\mathbf{r}_N) / \psi_T(\mathbf{r}_1,\mathbf{r}_2,\ldots,\mathbf{r}_N)$ within customary DMC [known as mixed estimation, $\varrho_{mix}(r)=\langle A(r)\rangle_{DMC}$].[48] However, a more accurate evaluation of $\varrho(r)$, known as extrapolated estimation, is given by the expression

$$\varrho(r) = 2\varrho_{mix}(r) - \varrho_{VMC}(r), \tag{14}$$

where $\varrho_{VMC}(r)$ results from averaging $A(\mathbf{r},\mathbf{r}_1,\ldots,\mathbf{r}_N)$ within the variational Monte Carlo approach. In Fig. 5, we plot our results for $\varrho(r)$ as given by Eq. (14). In the same figure, we also enclose the Gaussian curve $G(r)=e^{-br^2}$ [given that $\varrho(0)=1$], which best fits our calculations, with an optimal parameter value $b=5.743(36)$ Å^{-2}. In order to test the quality of this fit (which in the reduced χ^2 test gives the value 0.99), we have calculated the atomic kinetic energy of solid Ne through the formula

$$E_k = -\left[\frac{\hbar^2}{2m_{\mathrm{Ne}}}\nabla^2\varrho(r)\right]_{r=0}, \tag{15}$$

but assuming $G(r)$ instead of $\varrho(r)$. In fact, it may be shown that Eq. (15) derives from the kinetic-energy sum rule

$$E_k = \frac{\hbar^2}{2m_{\mathrm{Ne}}}\frac{1}{(2\pi)^3\rho}\int d\mathbf{k}\, k^2 n(k). \tag{16}$$

Proceeding so, we have obtained E_k=41.43(26) K, which fully agrees with the direct estimation 41.51(6) K. This finding allows us to conclude that $\varrho(r)$ in solid Ne at $T=0$ can be well considered Gaussian shaped at all effects.

We have also computed the atomic momentum distribution of solid Ne by taking the Fourier transform of $\varrho(r)$ over a set of k-vector points, as expressed in Eq. (13). In Fig. 6, we plot the results of these calculations (dots) and additionally the Fourier transform of the aforegiven Gaussian fit to $\varrho(r)$ (solid line with width signalizing the associated uncertainty). Obviously, once $\varrho(r)$ has proved Gaussian, $n(k)$ turns out to be of the same kind.

D. Degree of anharmonicity

The self-consistent phonon approach[29] has proved very accurate in characterizing solids in the middle way between classical and quantum behavior. Very essentially, this theory makes the assumption of particles coupled harmonically with frequencies and modes depending on the crystal symmetry and lattice parameter and which are determined through a self-consistent procedure. A simplified version of this

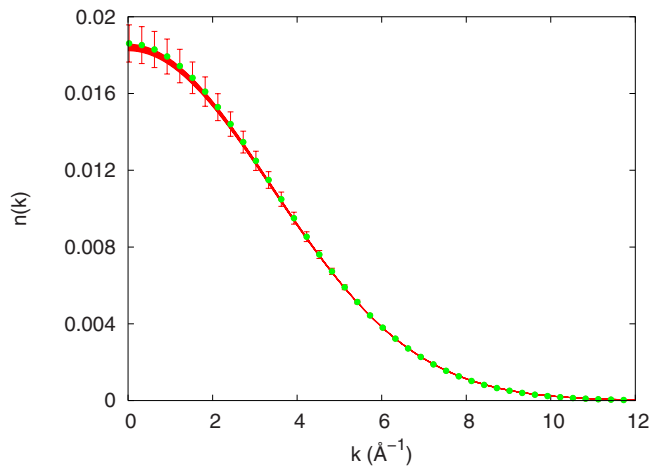

FIG. 6. (Color online) Momentum distribution of solid Ne at the equilibrium density (green dots and bars). The solid line in the figure corresponds to the Fourier transform of the Gaussian curve previously fitted to $\varrho(r)$ (the width of the line represents the uncertainty of the fit).

method is the self-consistent average phonon approach,[27,28] which adopts the expressions of the SCP approach but replacing the summation over the different vibrational frequencies by an averaged one: namely, the Einstein frequency Ω_0. Despite this crude simplification, the agreement between measurements and SCAP results for rare gase solids like Ar, Kr, and also Ne is excellent in what concerns thermodynamic properties (isothermal bulk modulus, specific heat, etc.).[45] However, we want to know to what extent harmonic assumptions in solid Ne are accurate enough for deriving microscopic properties of its ground state. With this aim, we have calculated the atomic kinetic energy and mean-squared displacement within SCAP through the formulas

$$\Omega_0^2 = \frac{1}{3m_{\mathrm{Ne}}N}\left\langle \sum_{i=1}^{N} \nabla_i^2 V_2(\mathbf{r}) \right\rangle \tag{17}$$

and

$$\langle \mathbf{u}^2 \rangle^{(\mathrm{SCAP})} = \frac{3\hbar}{2m_{\mathrm{Ne}}\Omega_0},$$

$$\langle E_k \rangle^{(\mathrm{SCAP})} = \frac{1}{2} m_{\mathrm{Ne}} \langle \mathbf{u}^2 \rangle^{(\mathrm{SCAP})} \Omega_0^2 = \frac{3}{4}\hbar\Omega_0, \tag{18}$$

where $V_2(r)$ is the Aziz HFD-B pair potential. We first compute the exact value of Ω_0 with the pure estimator technique within the DMC approach and then calculate the value of expressions (18). The results that we have obtained are $\hbar\Omega_0$=62.04(1)K, $\langle \mathbf{u}_{\mathrm{Ne}}^2 \rangle^{SCAP}$=0.058(3) Å^2, and $\langle E_k \rangle^{SCAP}$ =46.5(1) K, which disagree noticeably from the DMC values $\langle \mathbf{u}_{\mathrm{Ne}}^2 \rangle$=0.077(1) Å^2 and $\langle E_k \rangle$=41.51(6)K. This outcome reveals that crude simplifications made on the vibrational properties of solid Ne may lead to important inaccurracies on the quantum description of such crystal.

In a further step, we have devised an harmonic model[46] in which the interaction between particles is pairwise and reads

$$V_2^{\mathrm{harm}}(r_{ij}) = V_2(r_{0,ij}) + \frac{1}{2}(\mathbf{u}_i - \mathbf{u}_j)^{\mathrm{T}} \left(\frac{\partial^2 V_2}{\partial \mathbf{r}_{ij}\, \partial \mathbf{r}_{ij}} \right)_{r_{ij}=r_{0,ij}} (\mathbf{u}_i - \mathbf{u}_j), \tag{19}$$

where $V_2(r)$ is the Aziz HFD-B interaction, $\mathbf{u}_i$ is defined as $\mathbf{r}_i - \mathbf{R}_i$, and the terms $V_2(r_{0,ij})$ and $\left(\frac{\partial^2 V_2}{\partial \mathbf{r}_{ij} \partial \mathbf{r}_{ij}}\right)_{r_{ij}=r_{0,ij}}$ in the right-hand side of Eq. (19) are evaluated, only once, for the atoms in the perfect crystal configuration ($r_{0,ij} \equiv |\mathbf{R}_i - \mathbf{R}_j|$). This approach is equivalent to assuming the pair of atoms i and j coupled through an harmonic spring of constant equal to the second derivative of $V_2(r)$ evaluated at the equilibrium distance $r_{0,ij}$. Within the DMC method and with the pure estimator technique, we have computed the exact ground-state total and kinetic energies of this model, arriving at the values e_0^{harm}=−251.35(4) K and E_k^{harm}=35.1(3) K, which differ notably from the results obtained with the full Aziz HFD-B interaction.

The relative failure of the previous approximations allow us to conclude that traditional harmonic approximations in solid Ne are not adequate for an accurate evaluation of its microscopic properties. Aimed at yielding a rough estimation of the degree of anharmonicity of solid Ne and to finalize with this section, we now compare solid Ne with solid ^{4}He, the most anharmonic among all the crystals, by invoking the Debye model. In the Debye approach for solids, particles are assumed as noninteracting quantum harmonic oscillators which vibrate with frequencies within a spectrum that is top bounded by the Debye frequency ω_D. Consequently, the atomic kinetic energy is expressed as $E_k^D = (9/16)\Theta_D$, where Θ_D is the Debye temperature and is equal to $\hbar\omega_D$. It is readily shown that $\Theta_D = 9\hbar^2/4m\langle \mathbf{u}^2 \rangle$, which in the case of solid Ne at equilibrium turns out to be 70.3(9) K [here, we have used the value $\langle \mathbf{u}_{\mathrm{Ne}}^2 \rangle$=0.077(1) Å^2], which in turn leads to E_k^D=39.5(5) K. Next, we define the dimensionless parameter $\Gamma \equiv 1.0 - (E_k^D/E_k)$, which in fact vanishes for the case of a pure harmonic solid (Debye model) and it progressively increases towards unity as anharmonic effects develop larger. For solid Ne and ^{4}He at their respective zero-temperature equilibrium volumes, we assess the values Γ_{Ne}=0.05 and Γ_{He}=0.44, where for helium we have used the data found in Ref. 47. By comparing these two figures, one could claim that anharmonic effects in solid Ne are about one order of magnitude less substantial than in ^{4}He.

IV. DISCUSSION AND CONCLUSIONS

In this work, we report the calculation of the ground-state atomic kinetic energy, one-body density matrix, and momentum distribution of solid Ne by means of the DMC method and the realistic Aziz HFD-B pair potential. Our approach is proved to perform notably for this crystal, as is shown by the very good overall agreement obtained with respect to thermodynamic experimental data. Our value for the atomic kinetic energy of solid Ne at the equilibrium volume, E_k =41.51(6) K, is in accordance with the low-temperature experimental data found in Refs. 23 and 26 and also with previous PIMC calculations performed with the LJ and Aziz

HFD-C2 pairwise interactions.[22,23,25] However, our result does not agree with the results obtained by Peeks and coworkers (previous to the work of Timms *et al.*) based also on deep-inelastic neutron scattering measurements. We have calculated the one-body density function of solid Ne and shown that it perfectly fits to a Gaussian curve. Consequently, the atomic momentum distribution, which is evaluated by performing the Fourier transform of $\varrho(r)$, is of the same kind. Interestingly, Withers and Glyde[49] have shown very recently by means of simple models that the deviation of $n(k)$ from a Gaussian pattern in quantum solids may arise by effect of anharmonicity and/or the introduction of atomic exchanges. We have checked that anharmonic effects in the ground state of solid Ne are relevant by calculating some of its microscopic properties within traditional harmonic schemes and quoting significant discrepancies with respect to the full quantum results. It is noted that we have not attempted to include atomic exchange effects in the present work since *a priori* and very reasonably, these are not expected to play any substantial role in the ground state of solid Ne (contrarily to what may occur in ^{4}He, for instance). Even so, we do not appreciate, within the statistical uncertainty, any deviation from a Gaussian pattern in the $\varrho(r)$, or equivalently $n(k)$, of solid Ne; therefore, the degree of anharmonicity of Ne at zero temperature may be regarded as fairly moderate.

ACKNOWLEDGMENTS

We acknowledge financial support from DGI (Spain) Grant No. FIS2005-04181 and Generalitat de Catalunya Grant No. 2005GR-00779.

[1] G. L. Pollack, Rev. Mod. Phys. **36**, 748 (1964).
[2] M. L. Klein and A. Venables, *Rare Gas Solids* (Academic Press, London, 1976).
[3] J. P. Hansen and I. R. McDonald, *Theory of Simple Liquids* (Academic Press New York, 1976).
[4] E. Kim and M. H. W. Chan, Science **305**, 1941 (2004).
[5] Ann Sophie C. Rittner and J. D. Reppy, Phys. Rev. Lett. **97**, 165301 (2006).
[6] N. Prokof'ev and B. Svistunov, Phys. Rev. Lett. **94**, 155302 (2005).
[7] D. M. Ceperley and B. Bernu, Phys. Rev. Lett. **93**, 155303 (2004).
[8] R. T. Azuah, W. G. Stirling, H. R. Glyde, P. E. Sokol, and S. M. Bennington, Phys. Rev. B **51**, 605 (1995).
[9] R. T. Azuah, W. G. Stirling, H. R. Glyde, and M. Boninsegni, J. Low Temp. Phys. **109**, 287 (1997).
[10] S. O. Diallo, J. V. Pearce, R. T. Azuah, and H. R. Glyde, Phys. Rev. Lett. **93**, 075301 (2004).
[11] J. De Boer, Rep. Prog. Phys. **12**, 305 (1949).
[12] T. M. Hakim and H. R. Glyde, Phys. Rev. B **37**, 984 (1988).
[13] B. L. Hammond, W. A. Lester, Jr., and P. J. Reynolds, *Monte Carlo Methods in Ab initio Quantum Chemistry* (World Scientific, Singapore, 1994).
[14] R. Guardiola, in *Microscopic Quantum Many-Body Theories and Their Applications*, edited by J. Navarro and A. Polls (Springer, Berlin, 1998).
[15] D. M. Ceperley and M. H. Kalos, *Monte Carlo Methods in Statistical Physics* (Springer, Berlin, 1979).
[16] R. A. Aziz and M. J. Slaman, Chem. Phys. **130**, 187 (1989).
[17] N. Bernades, Phys. Rev. **112**, 1534 (1958).
[18] L. H. Nosanow and G. L. Shaw, Phys. Rev. **128**, 546 (1962).
[19] T. R. Koehler, Phys. Rev. Lett. **17**, 89 (1966).
[20] D. A. Peek, M. C. Schmidt, I. Fujita, and R. O. Simmons, Phys. Rev. B **45**, 9671 (1992).
[21] M. Asger and Q. N. Usmani, Phys. Rev. B **49**, 12262 (1994).
[22] A. Cuccoli, A. Macchi, V. Tognetti, and R. Vaia, Phys. Rev. B **47**, 14923 (1993).
[23] D. N. Timms, A. C. Evans, M. Boninsegni, D. M. Ceperley, J. Mayers, and R. O. Simmons, J. Exp. Zool. **8**, 6665 (1996).
[24] R. A. Aziz, W. J. Meath, and A. R. Allnatt, Chem. Phys. **79**, 295 (1983).
[25] M. Neumann and M. Zoppi, Phys. Rev. E **65**, 031203 (2002).
[26] D. N. Timms, R. O. Simmons, and J. Mayers, Phys. Rev. B **67**, 172301 (2003).
[27] K. S. Liu, M. H. Kalos, and G. V. Chester, Phys. Rev. A **10**, 303 (1974).
[28] P. J. Reynolds, R. N. Barnett, B. L. Hammond, and W. A. Lester, Jr., J. Stat. Phys. **43**, 1017 (1986).
[29] J. Casulleras and J. Boronat, Phys. Rev. B **52**, 3654 (1995).
[30] K. Shukla, A. Paskin, D. O. Welch, and G. J. Dienes, Phys. Rev. B **24**, 724 (1981).
[31] A. Paskin, A. M. Llois de Kreiner, K. Shukla, D. O. Welch, and G. J. Dienes, Phys. Rev. B **25**, 1297 (1982).
[32] H. R. Glyde, *Excitations in Liquid and Solid Helium* (Clarendon Press, Oxford, 1994).
[33] M. H. Kalos, D. Levesque, and L. Verlet, Phys. Rev. A **9**, 2178 (1974).
[34] S. A. Chin, Phys. Rev. A **42**, 6991 (1990).
[35] R. J. Hemley, C. S. Zha, A. P. Jephcoat, H. K. Mao, L. W. Finger, and D. E. Cox, Phys. Rev. B **39**, 11820 (1989).
[36] N. D. Drummond and R. J. Needs, Phys. Rev. B **73**, 024107 (2006).
[37] M. Grimsditch, P. Loubeyre, and A. Polian, Phys. Rev. B **33**, 7192 (1986).
[38] V. F. Lotrich and K. Szalewicz, Phys. Rev. Lett. **79**, 1301 (1997).
[39] L. H. Nosanow, Phys. Rev. Lett. **13**, 270 (1964).
[40] J. P. Hansen and D. Levesque, Phys. Rev. **165**, 293 (1968).
[41] J. P. Hansen, Phys. Lett. **30A**, 214 (1969).
[42] G. T. McConville, J. Chem. Phys. **60**, 4093 (1974).
[43] D. N. Batchelder, D. L. Losee, and R. O. Simmons, Phys. Rev. **162**, 767 (1967).
[44] C. P. Herrero, Phys. Rev. B **68**, 172104 (2003).
[45] P. Mohazzabi and F. Behroozi, Phys. Rev. B **36**, 9820 (1987).
[46] D. C. Wallace, *Thermodynamics of Crystals* (Wiley, New York, 1972).
[47] C. Cazorla and J. Boronat, J. Phys.: Condens. Matter **20**, 015223 (2008).
[48] S. Moroni, G. Senatore, and S. Fantoni, Phys. Rev. B **55**, 1040 (1997).
[49] B. Withers and H. R. Glyde, J. Low Temp. Phys. **147**, 633 (2007).